Quantitative Analyses of Pediatric Cervical Spine Ossification Patterns Using Computed Tomography

Narayan Yoganandan, PhD, Frank A. Pintar, PhD, Sean M. Lew, MD
Department of Neurosurgery, Medical College of Wisconsin, Milwaukee, WI, USA

Raj D. Rao, MD
Department of Orthopaedic Surgery, Medical College of Wisconsin, Milwaukee, WI, USA

Nagarajan Rangarajan, PhD
GESAC Incorporated, Boonsborough, MD, USA

ABSTRACT – The objective of the present study was to quantify ossification processes of the human pediatric cervical spine. Computed tomography images were obtained from a high resolution scanner according to clinical protocols. Bone window images were used to identify the presence of the primary synchondroses of the atlas, axis, and C3 vertebrae in 101 children. Principles of logistic regression were used to determine probability distributions as a function of subject age for each synchondrosis for each vertebra. The mean and 95% upper and 95% lower confidence intervals are given for each dataset delineating probability curves. Posterior ossifications preceded bilateral anterior closures of the synchondroses in all vertebrae. However, ossifications occurred at different ages. Logistic regression results for closures of different synchondrosis indicated p-values of <0.001 for the atlas, ranging from 0.002 to <0.001 for the axis, and 0.021 to 0.005 for the C3 vertebra. Fifty percent probability of three, two, and one synchondroses occurred at 2.53, 6.97, and 7.57 years of age for the atlas; 3.59, 4.74, and 5.7 years of age for the axis; and 1.28, 2.22, and 3.17 years of age for the third cervical vertebrae, respectively. Ossifications occurring at different ages indicate non-uniform maturations of bone growth/strength. They provide an anatomical rationale to reexamine dummies, scaling processes, and injury metrics for improved understanding of pediatric neck injuries

INTRODUCTION

The human pediatric spine grows with age. In general, the age group between the newborn to one year can be skeletally represented by three primary ossification centers (Figure 1a). The age group between one and three years can be represented by the fusion of the posterior synchondrosis. The age group between three and six years signifies fusion of primary ossification centers (Yoganandan et al., 1998). Although textbooks describe ossification, quantifications on the development of vertebrae in terms of probability distributions are not available (Bailey, 1952, Bird and Darling, 2001, Clark, 1998, Ganey and Ogden, 2001, Lew and Kaufman, 2008, Sherk and Parke, 1989, Weinstein, 1994, Williams, 1995, Yoganandan et al., 2001, Yoganandan et al., 2008). Because vertebral ossification is directly correlated to growth, strength, and spinal stability, it is important to quantify ossification patterns (Cusick and Yoganandan, 2002). The present study is focused on this objective. A brief description is given of the ossification processes.

CORRESPONDING AUTHOR:
Narayan Yoganandan, PhD, Department of Neurosurgery, Medical College of Wisconsin, 9200 West Wisconsin Avenue, Milwaukee, WI, 53226, USA; Email: yoga@mcw.edu

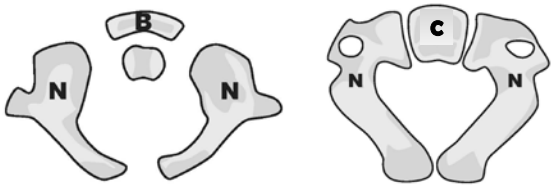

Figure 1a: Axial views of C1 and C2 vertebra (left and right) showing the synchondroses (shown as gaps) between the ossification centers (N: neurocentral, B: anterior arch, C: centrum). In the axial view, C3 vertebra also appears similar to C2 with the same ossification centers, and hence, not included.

CERVICAL SPINE OSSIFICATIONS

The structural components of the osteoligamentous cervical spine include the seven vertebrae and their interconnecting tissues. The first two vertebrae are termed the atlas and axis, and the remaining three-to-seven are typical, termed C3 to C7. Intervertebral discs start from the axis, ligaments interconnect from the base of the skull to C7, and the spinal cord originating from the foramen magnum is housed in the osteoligamentous column (Bick, 1961, Bick and Copel, 1950, Carpenter, 1961, Chung et al., 1976,

Coventry et al., 1945, Dickerson and Dobbing, 1966, Gilsanz et al., 1988, Haas, 1939, Hallen, 1962, Hirsch et al., 1967, Kasai, 1998, Kasai et al., 1996, Knutsson, 1961, Markuske, 1977, Oda et al., 1988, Ogden et al., 1994, Ogden et al., 1987, Peacock, 1956, Roaf, 1960, Taylor, 1970, Walmsley, 1953). Developmental anatomies relevant to the present study are the atlas, axis, and C3.

Atlas (C1)

The first vertebra (C1), the atlas, forms out of three primary ossification centers; one occurs in the anterior region and two occur bilaterally in the posterior neural arches. Anatomical textbooks qualitatively suggest that the former center develops several months after birth and the other two centers are present at the time of birth (Weinstein, 1994). The junction between the anterior arch and the bilateral posterior arches are called the neurocentral synchondroses (Lew and Kaufman, 2008). The two neural arches fuse or join dorsally in the midline at the posterior synchondrosis. Fusion of the posterior synchondrosis is generally followed by fusion of the neurocentral synchondroses. The spinal canal fully forms and attains the mature adult size following complete fusion of the primary ossification process (Hinck et al., 1962, Tulsi, 1971, Yousefzadeh et al., 1982).

Axis (C2)

The second vertebra (C2), the axis, forms from five primary ossification centers (Bailey, 1952, Herkowitz et al., 2011, O'Rahilly and Benson, 1985, Ogden et al., 1987, Verbout, 1985, Weinstein, 1994). One occurs in the centrum, two occur bilaterally in the posterior neural arches, and two occur bilaterally in the odontoid process. The two centers in the odontoid are joined at birth. The odontoid process is connected to the body of the axis by dentocentral synchondrosis. Paired neurocentral synchondroses form the connection between the two posterior arches and centrum. Development of the ossification process is such that the neural arches fuse posteriorly, followed by fusion of the centrum-neural arch and odontoid process-centrum. The spinal canal reaches its mature size following closure of the posterior and neuro-central synchondroses (Hinck et al., 1962, Tulsi, 1971, Yousefzadeh et al., 1982). However, the dento-central synchondrosis continues to mature, and in some children, the ossification process never completes.

Third cervical vertebra (C3)

Each of the remaining five vertebrae (C3-C7) forms from three primary ossification centers; one in the anterior centrum and two in the posterior neural arches (Bailey, 1952, Chandraraj and Briggs, 1991, Clark, 1998, Ford et al., 1982, O'Rahilly and Benson, 1985, Ogden et al., 1987, Verbout, 1985, Weinstein, 1994). The neurocentral synchondrosis is the joining element between the neural arches and the centrum. The two neural arches are interconnected by the posterior synchondrosis. The progression of the ossification process is such that the neural arches join posteriorly, followed by the closure of the neurocentral synchondroses. The spinal canal attains the final adult size after completion of the primary ossifications, like the atlas and axis (Hinck et al., 1962, Tulsi, 1971, Yousefzadeh et al., 1982).

As briefly stated in the introduction, the purpose of the present study was to quantify the ossification patterns of the atlas, axis, and the third cervical vertebrae in the growing human spine and express the output in terms of probability distributions.

METHODS

Subject selection

The retrospective research study was approved by the Institutional Review Board of the Children's Hospital of Wisconsin, the organization responsible for such approvals in our medical center campus at the Medical College of Wisconsin. According to the United States Government Health Insurance Portability and Accountability Act, de-identified records were used in the present study (1996).

All data were obtained from a Pediatric Level One Trauma Center, serving Southeastern Wisconsin. The Children's Hospital of Wisconsin is the only Pediatric Level One Trauma Center in the region. Cervical spine radiographs and helical CT scans were obtained as part of routine imaging evaluations of pediatric patients presenting to the emergency room. Most of these scans were obtained to rule out traumatic injuries. Patients with demonstrable clinical evidence of congenital or developmental disease, neoplastic growth, adverse neurological conditions, vertebral and muscular abnormalities, fracture/dislocation, epiphyseal injury, spine surgery, and scoliosis, that might affect normal vertebral growth, were deemed to be inappropriate, and hence, excluded from the study. The majority of the population underwent imaging to exclude cervical injury after trauma.

Imaging

A high resolution CT scanner (Somatom Plus 4; Siemens, Erlangen, Germany) was used to obtain

spine images at 2.5 mm intervals according to established clinical protocols. In-plane resolution was 512x512 pixels. The scanner was calibrated according to hospital requirements including daily fast calibrations, weekly water phantom quality assurance, quarterly American College of Radiology (ACR) phantom testing, quarterly performance maintenance done by the manufacturer, and in addition, annual system performance evaluations were conducted by physicians at the Medical College of Wisconsin. Axial and sagittal images obtained as a part of the screening protocol were available for quantitative analyses. Standard bone windows (width: 2000, level: 400 Hounsfield units) were used to identify the presence or absence of synchondroses. The presence of synchondroses of the atlas, axis, and C3 vertebrae were identified between the ossification centers: two anteriorly between the neural arches and centrum, and one posteriorly at the midline from the fusion of the neural arches. Synchondroses were associated with changes in radiographic density. Analyses of the presence of synchondroses for the various vertebrae were done using logistic regression, and the probability distributions as a function of subject age are presented for all vertebrae and for the different synchondrosis. Age was treated as a continuous variable. The average and 95% upper and lower confidence interval data are used to illustrate probability curves. The terms "children," "patients," and "subjects" are used synonymously in this paper.

RESULTS

As this was a retrospective review, the study included only patients meeting the inclusion-exclusion criteria stated in the methods section. In other words, the query was not setup to collect all patient records and then sort through those who met the criteria. Instead, it was designed to only obtain CT scans from patients with normal cervical anatomy. Furthermore, as this was not an epidemiological-type study, it was not important to gather the size of the total ensemble. Figure 1b shows CT scans with and without the presence of synchondroses.

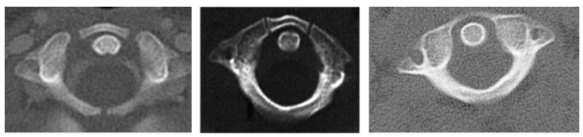

Figure 1b: CT scan of C1 showing the presence of three (left), two (right), and no synchondrosis.

Data from 101 children were available to quantify the ossification patterns of the atlas (C1), axis (C2), and C3 vertebrae. The demographics of the ensemble was such that subject age ranged from four months to eighteen years, with a mean of age of 7.9 years (standard deviation: ± 5.7 years). There were 33 females (mean age: 7.3 ± 6.1 years) and 68 males (mean age: 8.2 ± 5.5 years). Figure 1c shows the sample size distribution on an annual age basis. Logistic regression analyses of ossification data for all vertebrae indicated significant p values (Table 1). Vertebra-specific results are given.

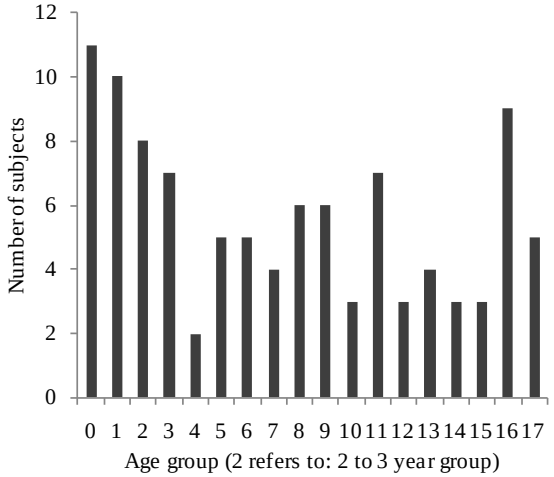

Figure 1c - Bar chart illustrating the sample sizes of 101 subjects on an annual age basis.

Table 1 – P values from logistic regression

Level	Synchondroses		
	1	2	3
Atlas (C1)	< 0.001	< 0.001	< 0.001
Axis (C2)	< 0.001	< 0.001	= 0.002
C3	= 0.003	= 0.005	= 0.021

Atlas (C1 vertebra)

The probability distributions of the presence of at least one, two, and three synchondroses for the atlas as functions of subject age in years are shown in figure 2, 3, and 4, respectively. Logistic regression analysis indicated that 50% probabilities of three, two, and one synchondrosis occur at 2.53, 6.97, and 7.57 years of age, respectively. Table 2 summarizes data associated with 25, 50, and 75% probabilities.

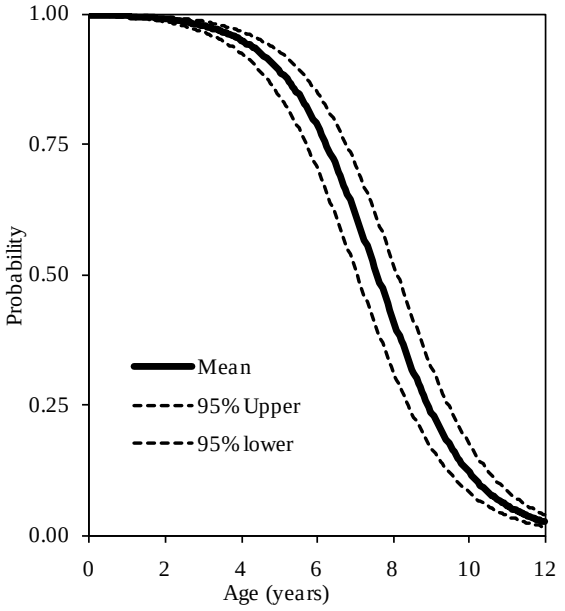

Figure 2 - Logistic regression curves illustrating the presence of one synchondrosis at the C1 level. Upper and lower bounds are also shown.

Table 2 – Synchondrosis probabilities for the atlas as a function of age (years)

Synchondroses	Probability at % level		
	25	50	75
1	8.92	7.57	6.23
2	8.59	6.97	5.36
3	4.27	2.53	0.79

Axis (C2 vertebra)

The probability distributions of the presence of at least one, two, and three synchondroses for the axis as functions of subject age in years are shown in figure 5, 6, and 7, respectively. Logistic regression analysis indicated that 50% probabilities of three, two, and one synchondrosis occur at 3.59, 4.74, and 5.7 years of age, respectively. Table 3 summarizes data associated with 25, 50, and 75% probabilities.

Table 3 – Synchondrosis probabilities for the axis as a function of age (years)

Synchondroses	Probability at % level		
	25	50	75
1	7.29	5.70	3.75
2	5.92	4.64	2.03
3	4.54	3.59	0.31

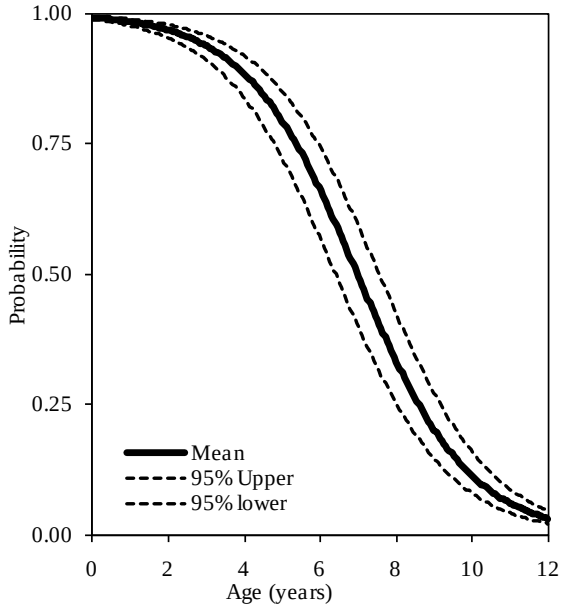

Figure 3 - Logistic regression curves illustrating the presence of two synchondroses at the C1 level. Upper and lower bounds are shown.

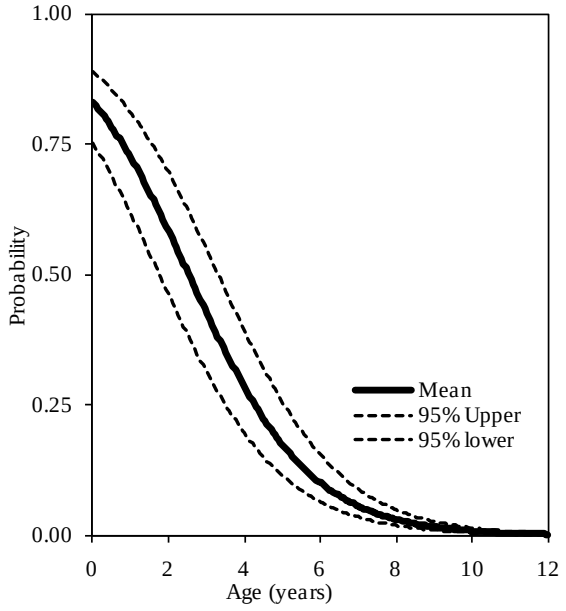

Figure 4 - Logistic regression curves illustrating the presence of three synchondroses at the C1 level. Upper and lower bounds are shown.

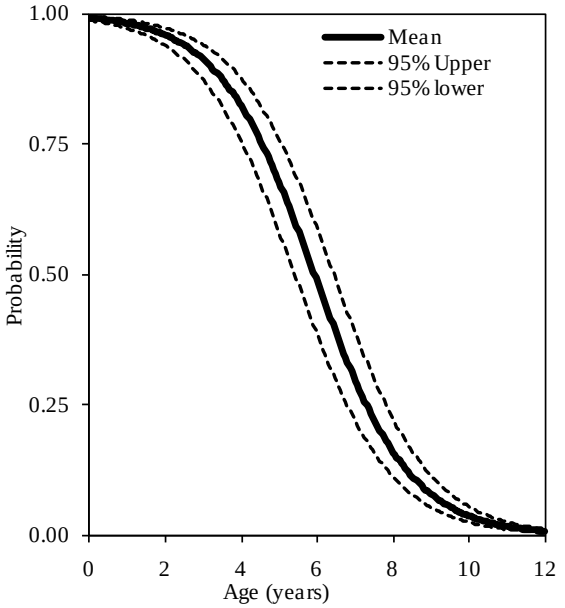

Figure 5 - Logistic regression curves illustrating the presence of one synchondrosis at the C2 level. Upper and lower bounds are shown.

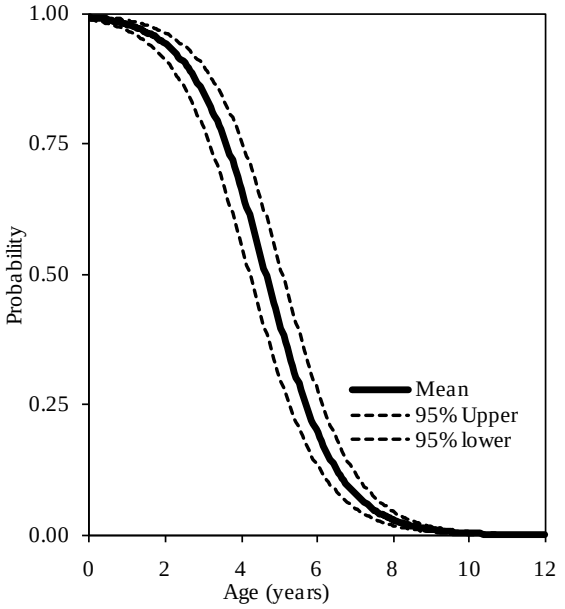

Figure 6 - Logistic regression curves illustrating the presence of two synchondroses at the C1 level. Upper and lower bounds are shown.

C3 vertebra

The probability distributions of the presence of at least one, two, and three synchondroses for the axis as functions of subject age in years are shown in figure 8, 9, and 10, respectively. Logistic regression analysis indicated that 50% probabilities of three, two, and one synchondrosis occur at 1.28, 2.22, and 3.17 years of age, respectively. Table 4 summarizes data associated with 25, 50, and 75% probabilities.

Table 4 – Synchondrosis probabilities for the C3 vertebra as a function of age (years)

	Probability at % level		
Synchondroses	25	50	75
1	3.60	3.17	0.93
2	2.52	2.22	0.65
3	1.45	1.28	0.37

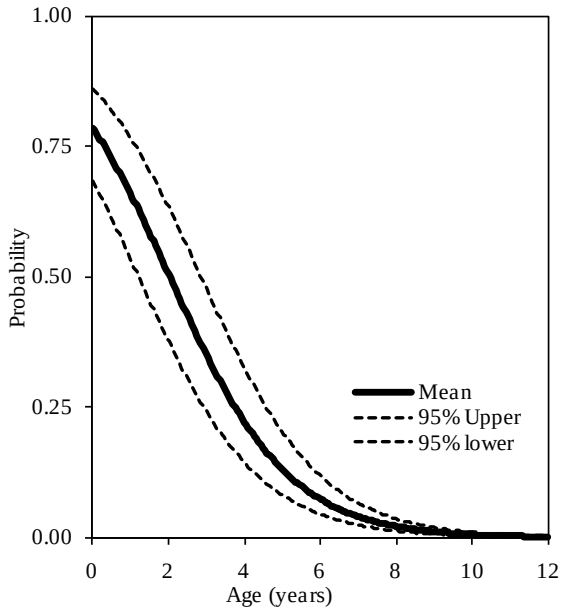

Figure 7 – Logistic regression curves illustrating the presence of three synchondroses at the C2 level. Upper and lower bounds are shown.

DISCUSSION

As indicated in the Introduction, the aim of this study was to quantify ossification processes of pediatric human cervical spine vertebrae. In the living human, this can be accomplished using conventional x-rays, CT, or magnetic resonance imaging (MRI). Computed tomography images were used due to its superiority over MRI for bone-related measurements (Ford et al., 1982, Yoganandan et al., 1998). CT is also superior to traditional x-rays as radiographs capture an integrated image of the three-dimensional spine (not limited to scan thickness like CT), and axial views of the spine are less than adequate for quantitative analyses (Yoganandan et al., 2006, Yoganandan et al., 2006).

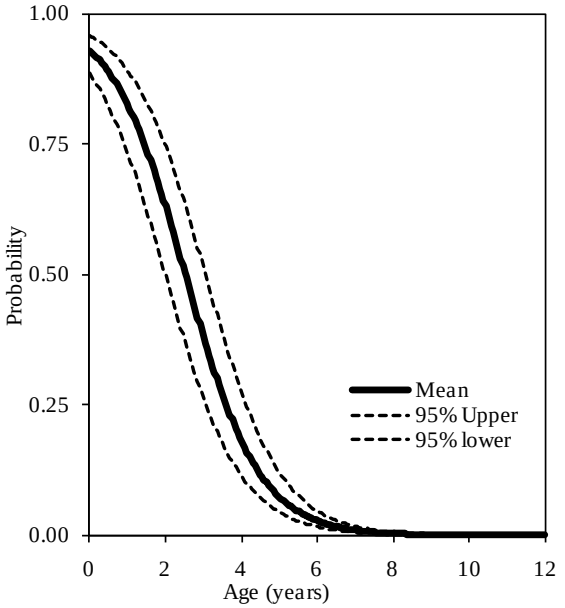

Figure 8 - Logistic regression curves illustrating the presence of one synchondrosis at the C3 level. Upper and lower bounds are shown.

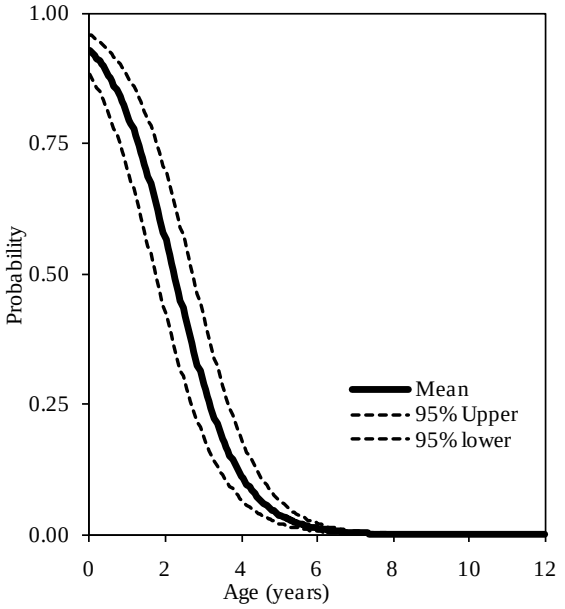

Figure 9 - Logistic regression curves illustrating the presence of two synchondroses at the C3 level. Upper and lower bounds are shown.

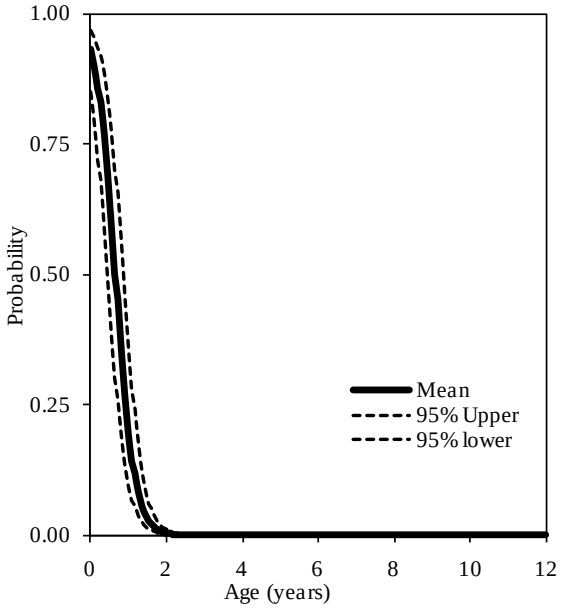

Figure 10 – Logistic regression curves illustrating the presence of three synchondroses at the C3 level. Upper and lower bounds are also shown.

Denuded vertebrae from cadavers have been used to determine the morphological characteristics of the human spine (Francis, 1955). A cadaveric spine can be multiply imaged (MRI, CT, X-ray, DEXA etc), tissue histology can be performed, and testing on a structural and material basis can be performed. However, it was not feasible to use the cadaver model due to constraints in obtaining pediatric spines, and more importantly, cartilaginous structures accounting for the ossification processes lose integrity in the ex vivo environment. Furthermore, the use of CT images is clinical, and quantitative data extracted from this process may be applicable to clinicians towards an improved understanding of the developmental processes of the child neck.

Although not pertinent to this synchondroses-based study, the mean anterior ring heights of the C1 vertebrae were: 0.76 cm in the 0-3 year, 0.77 cm in the 3-6 year; 0.89 cm in the 6-9 year, 1.02 cm in the 9-12-year groups; 1.04 cm in the 12-15 year, and 1.15 cm in the 15-18 year groups. The mean posterior ring heights had a similar distribution: 0.63, 0.58, 0.74, 1.0, 0.85, and 1.19 cm in the 3-6 year, 6-9 year, 9-12 year, 12-15 year, and 15-18 year groups, respectively. Other data can also be extracted from these images.

Partial volume effect is inherent to CT. This was not quantitatively explored in the present retrospective

study. To minimize these effects, the assessment of ossification was done by spine surgeons, and synchondroses were generally visible in more than one slice. Since the objective of the study was to identify the presence or absence of synchondroses, any potential volume averaging artifact was considered minimal. Furthermore, in general, the imaging plane was perpendicular to the plane of synchondroses. Hence, these anatomical (synchondrosis) - and image (CT issue)-related features tend to minimize the artifact.

The present study provided ossification-related data for the three upper cervical vertebrae although the human neck consists of seven vertebrae with interconnecting soft tissues from the basilar skull to the thoracic spine (Yoganandan et al., 1998, Yoganandan et al., 1996). While this appears to be a limitation, as a first step, findings from C3 vertebrae are considered to be applicable to C4 to C7 levels. This is because ossification processes are almost identical in the C3-C7 spinal region (Lew and Kaufman, 2008). These lower vertebrae were not included in the present analyses because the study was retrospective, and the lower cervical spine images were not routinely obtained in all cases at the time the patient was treated. Further, all images were patient- instead of volunteer-based. It is not clinically common to obtain CT scans inferior to C3 unless suspicion arises due to abnormality, dysfunction, or instability of the cervical spinal column (Kokabi et al., 2011). Patients with such potential abnormalities were excluded, as described in the methods section.

Further, inclusion of vertebrae inferior to C3 during CT scanning exposes patients to additional radiation (Baumann et al., 2010, Dorfman et al., 2011). It is well known that the awareness of the risk of exposure increased following investigations from the United States Food and Drug Administration in 2009. Recent medical and epidemiological literatures have been quantifying such data (Brenner, 2010, Brunetti et al., 2010, Mahesh, 2010, Tsalafoutas and Koukourakis, 2010). Hence, human volunteers were not enrolled specifically for this study, and IRB approval was obtained for only the retrospective analysis.

A traditional approach to determine the closure of synchondroses, representing ossification patterns, is to follow the same subject on a longitudinal basis. This approach has been adopted to quantify spinal and other bone measurements in boys and girls (Kalkwarf et al., 2007). Dual energy x-ray absorptiometric techniques have been used. This method cannot be used for the upper cervical spine. Exposing healthy and normal human volunteers, especially at younger ages and during puberty, to radiation is an issue with CT. Although conventional x-rays pose significantly reduced risk compared to CT, ossification is not amenable to the same degree of determination. Consequently, the present study incorporated the methodology of retrieving retrospective (instead of longitudinal), normal patient data without exposing subjects to additional radiation risk, for determining age-specific probability distributions. At the same time, the most appropriate imaging technique, CT scans, were used to obtain quantitative data to perform logistic regression analyses.

As also indicated in the Introduction, the anatomic literature has been generally qualitative in terms of the development of human vertebral ossification patterns (Herkowitz et al., 2011, Lew and Kaufman, 2008, Weinstein, 1994). To the best knowledge of the authors, probability distributions of the ossification processes of human vertebrae have not been reported (Hilker et al., 2002, Jebaseelan et al., 2010, Kumaresan et al., 1997, Kumaresan et al., 2000, Yoganandan et al., 2008). Descriptive statistical information such as mean and standard deviations are common in pediatric biomechanics and automotive medicine. For example, citing the need to gather data from younger children (under 8 years of age) ranges of motions of 67 subjects from 3 to 12 years of age were described using these measures under flexion-extension, lateral bending and "horizontal" rotation modes (Arbogast et al., 2007). In contrast, the current results provide normative data in terms of regression-based curves along with 95% confidence intervals.

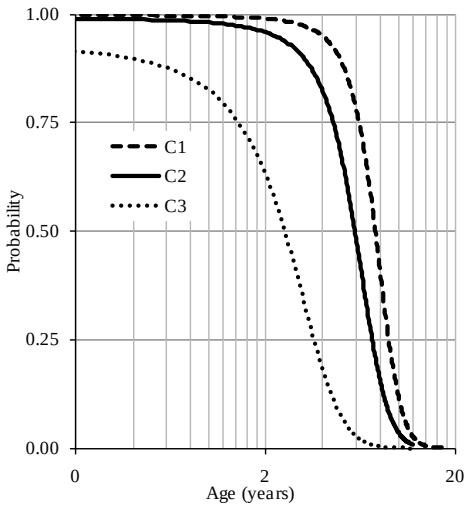

Figure 11 – Composite logistic regression curves illustrating completions of the posterior ossification for the three upper cervical vertebrae with age (log scale). Mean curves are shown for comparison.

An examination of probability distributions for the three vertebrae indicated similarities and differences. The posterior ossification was complete before the closure of the anterior synchondroses in all vertebrae, although the time of completion progressed from the caudal vertebra (Figure 11). Approximately seven, five, and two years of age were associated with 50% probability of closure of the posterior synchondroses in the atlas, axis, and C3 vertebrae. This implies that the caudal regions mature from the dorsal region, prior to the upper levels of the cervical spine (Ford et al., 1982). The caudo-cephalad ossification initiation is congruent with clinical literature (Clark, 1998). It should be noted that the fundamental developmental and biological processes of all spine vertebrae are similar as osteoblast activity responsible for bone formation is not site-specific (Williams, 1995). Earlier closure of the posterior synchondrosis confines the spinal canal dorsally and may be responsible for posterior vertebral alignment of the cervical column.

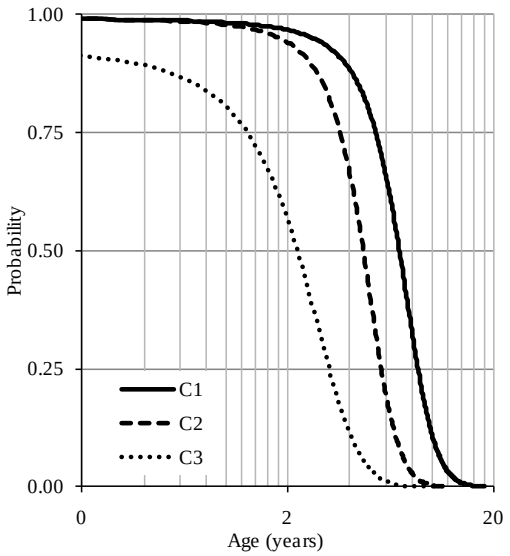

Figure 12 – Composite logistic regression curves illustrating completions of the neuro-central and posterior ossifications for the upper cervical vertebrae with age (log scale). Mean curves are shown for comparison.

The closure of the other two synchondroses also followed a similar pattern, caudo-cephalad, shown in figure 12. Approximately eight, six, and three years of age were associated with 50% probability of the closure of primary synchondroses in the atlas, axis and C3 vertebrae, respectively. These periods followed posterior ossifications (Figure 11). This time course of maturation is in general agreement with literature although no quantitative distributions are available. For example, it has been reported that, by three to four years of age, the posterior and bilateral neurocentral synchondroses are fused in the atlas, (Ogden et al., 1987). These closures occurred for the other two vertebrae between four to seven years of age (Lew and Kaufman, 2008). The primary maturity of the osseous anatomy and spinal canal size are fully established at these ages, allowing for the resistance of physiological loads such as eccentric compression-flexion forces from day-to-day activities (Yoganandan et al., 1998). This finding regarding the maturity of the canal size is also supported by literature; it has been reported that the canal reaches the adult size before six years of age and following the closure of the synchondroses (Ogden et al., 1987). Although not specific to this study, muscles play a role in the maturation process of the cervical spine.

CONCLUSIONS

This study quantified ossification processes of the atlas, axis, and the third cervical vertebrae of the growing human spine using CT images from 101 subjects. Logistic regression techniques were used to obtain probability distributions. Results indicated that the posterior ossification completes prior to the closure of the anterior neuro-central synchondroses in all vertebrae. Completion of ossification occurred at C3, followed by the axis, and then, the atlas. Approximately seven, five, and two years of age were associated with 50% probability of closure of the posterior synchondroses of the atlas, axis, and C3 vertebrae. Approximately eight, six, and three years of age were associated with 50% probability of primary ossification of the atlas, axis, and C3 vertebrae. Ossifications occurring at different ages indicate non-uniform maturations of bone growth/strength; thus offering an anatomical rationale to reexamine dummies, scaling processes, and injury metrics for improved understanding of pediatric neck injuries.

ACKNOWLEDGMENTS

The study was supported by VA Medical Research and the Department of Neurosurgery at the Medical College of Wisconsin. The authors acknowledge Dr. Mohit Maheshwari, of the Children's Hospital of Wisconsin for radiological assistance in the study.

REFERENCES

1996. Health Insurance Portability and Accountability Act: http://www.hipaa.org/.

Arbogast KB, Gholve PA, Friedman JE, Maltese MR, Tomasello MF, Dormans JP, 2007. Normal

cervical spine range of motion in children 3-12 years old. Spine (Phila Pa 1976) 32(10), E309-15.
Bailey D, 1952. The normal cervical spine in infants and children. Radiology 59, 712-719.
Baumann BM, Chen EH, Mills AM, Glaspey L, Thompson NM, Jones MK, Farner MC, 2010. Patient Perceptions of Computed Tomographic Imaging and Their Understanding of Radiation Risk and Exposure. Ann Emerg Med,
Bick EM, 1961. Vertebral growth; its relation to spinal abnormalities in children. Clin Orthopedics 21, 43-48.
Bick EM, Copel JW, 1950. Longitudinal growth of the human vertebra: a contribution to human osteogeny. J Bone Joint Surg 32-A(4), 803-814.
Bird S, Darling C, 2001. Postnatal maturation of the spine. In: D. McLone, ed. Pediatric Neurosurgery: Surgery of the developing nervous system. WB Saunders, Philadelphia, PA, 112-114.
Brenner DJ, 2010. Should we be concerned about the rapid increase in CT usage? Rev Environ Health 25(1), 63-8.
Brunetti MA, Mahesh M, Nabaweesi R, Locke P, Ziegfeld S, Brown R, 2010. Diagnostic Radiation Exposure in Pediatric Trauma Patients. J Trauma,
Carpenter EB, 1961. Normal and abnormal growth of the spine. Clinical Orthopedics 21(1), 49-55.
Chandraraj S, Briggs C, 1991. Muliple growth cartilages in the neural arch. The Anatomical Record 230, 114-120.
Chung MK, Batterman SC, Brighton CT, 1976. Shear strength of the human femoral capital epiphyseal plate. J Bone Jt Surgery 58A(1), 94-103.
Clark CR, 1998. The Cervical Spine. (Third ed.) Lippincott-Raven, Philadelphia, PA, 1003 pp.
Coventry MB, Ghormley RK, Kernohan JW, 1945. The intervertebral disc: its microscopic anatomy and pathology. Part I. Anatomy, development, and physiology. J Bone Joint Surg 27(1), 105-112.
Cusick JF, Yoganandan N, 2002. Biomechanics of the cervical spine 4: major injuries. Clin Biomech (Bristol, Avon) 17(1), 1-20.
Dickerson J, Dobbing J, 1966. Prenatal and postnatal growth and development of the central nervous system of the pig. Proc Royal Soc of London 166B, 384-395.
Dorfman AL, Fazel R, Einstein AJ, Applegate KE, Krumholz HM, Wang Y, Christodoulou E, Chen J, Sanchez R, Nallamothu BK, 2011. Use of Medical Imaging Procedures With Ionizing Radiation in Children: A Population-Based Study. Arch Pediatr Adolesc Med,
Ford DM, McFadden KD, Bagnall KM, 1982. Sequence of ossification in human vertebral neural arch centers. Anat Rec 203(1), 175-8.
Francis CC, 1955. Dimensions of the cervical vertebrae. Anat Rec 122(4), 603-9.
Ganey T, Ogden J, 2001. Development and maturation of the axial skeleton. In: S. Weinstein, ed. The Pediatric Spine. Williams and Wilkins, Philadelphia, PA, 3-54.
Gilsanz V, Gibbens DT, Roe TF, Carlson M, Senac MO, Boechat MI, Huang HK, Schulz EE, Libanati CR, Cann CC, 1988. Vertebral bone density in children: effect of puberty. Radiology 166(3), 847-50.
Haas SL, 1939. Growth in length of vertebrae. Arch Surg 38, 245-249.
Hallen A, 1962. Collagen and ground substance of human intervertebral disc at different ages. Acta Chem Scand 16(3), 705-710.
Herkowitz H, Garfin S, Eismont F, Bell G, Balderston R, 2011. Rothman-Simeone: The Spine. WB Saunders, Philadelphia, 2096.
Hilker CE, Yoganandan N, Pintar FA, 2002. Experimental determination of adult and pediatric neck scale factors. Stapp Car Crash J 46, 417-29.
Hinck V, Hopkins C, Savara B, 1962. Sagittal diameter of the cervical spinal canal in children. Radiol 79, 97-108.
Hirsch C, Schajowicz F, Galante J, 1967. Structural changes in the cervical spine: A study on autopsy specimens in different age groups. Acta Orthop, Scandinavia S109
Jebaseelan DD, Jebaraj C, Yoganandan N, Rajasekaran S, 2010. Validation efforts and flexibilities of an eight-year-old human juvenile lumbar spine using a three-dimensional finite element model. Med Biol Eng Comput 48(12), 1223-31.
Kalkwarf HJ, Zemel BS, Gilsanz V, Lappe JM, Horlick M, Oberfield S, Mahboubi S, Fan B, Frederick MM, Winer K, Shepherd JA, 2007. The bone mineral density in childhood study: bone mineral content and density according to age, sex, and race. J Clin Endocrinol Metab 92(6), 2087-99.
Kasai T, 1998. Growth of neck muscle in normal children at MR imaging.
Kasai T, Ikata T, Katoh S, Miyake R, Tsubo M, 1996. Growth of the cervical spine with special reference to its lordosis and mobility. Spine 21(18), 2067-2073.
Knutsson F, 1961. Growth and differentiation of the postnatal vertebra. Acta Radiologica 55, 401-408.
Kokabi N, Raper DM, Xing M, Giuffre BM, 2011. Application of imaging guidelines in patients with suspected cervical spine trauma: retrospective analysis and literature review. Emerg Radiol 18(1), 31-8.
Kumaresan S, Yoganandan N, Pintar F, 1997. Age-specific pediatric cervical spine biomechanical

responses: Three-dimensional nonlinear finite element models. In: Proceedings of the Stapp Car Crash Conf, Orlando, FL, 31-61.

Kumaresan S, Yoganandan N, Pintar FA, Maiman DJ, Kuppa S, 2000. Biomechanical study of pediatric human cervical spine: a finite element approach. J Biomech Eng 122(1), 60-71.

Lew S, Kaufman B, 2008. Neural and Vertebral Column Embryogenesis. In: D. Kim, R. Betz, S. Huhn and P. Newton, eds. Surgery of the Pediatric Spine. Thieme, New York, NY, 1-10.

Mahesh M, 2010. Medical radiation exposure with focus on CT. Rev Environ Health 25(1), 69-74.

Markuske H, 1977. Sagittal diameter measurements of bony cervical spinal canal in children. Pediat Radiol 6, 129-131.

O'Rahilly R, Benson DR, 1985. The development of the vertebral column. In: D.S. Bradford and R.N. Hensinger, eds. The Pediatric Spine. Thieme Inc., New York, 3-17.

Oda J, Tanaka H, Tsuzuki N, 1988. Intervertebral disc changes with aging of human cervical vertebra - from neonate to 80s. Spine 13(11), 1205-1211.

Ogden J, Ganey T, Sasse J, Neame P, Hilbelink D, 1994. Development and maturation of the axial skeleton. In: S. Weinstein, ed. The Pediatric Spine: Principles and Practice. Raven Press, New York, 1959.

Ogden JA, Grogan DP, Light TR, 1987. Postnatal development and growth of musculoskeletal system. In: J. Albright and R. Brand, eds. The Scientific Basis of Orthopaedics. Appleton & Lange, CA, 526.

Peacock A, 1956. Observations on the postnatal structure of the intervertebral disc in man. J Anat 86(Part 2), 162-179.

Roaf R, 1960. Vertebral growth and its mechanical control. J Bone Joint Surg 42B, 40-59.

Sherk H, Parke W. eds, 1989, "Developmental Anatomy," Lippincott, Philadelphia, PA, The Cervical Spine; 881 pp.

Taylor J, 1970. Growth of human intervertebral disc. J Anat 107, 183-184.

Tsalafoutas IA, Koukourakis GV, 2010. Patient dose considerations in computed tomography examinations. World J Radiol 2(7), 262-8.

Tulsi RS, 1971. Growth of the human vertebral column: an osteological study. Acta Anat 79, 570-580.

Verbout A, 1985. Development of the vertebral column. Adv Anat Embryol Cell Biol 90, 1-100.

Walmsley R, 1953. Development and growth of the intervertebral disc. Edinburgh Medical Journal LX(8), 341-364.

Weinstein S, 1994. Pediatric spine: Principles and Practice. Raven Press, New York, 1959.

Williams PL, 1995. Gray's Anatomy. Churchill Livingstone, New York, 2092.

Yoganandan N, Kumaresan S, Pintar F, Gennarelli T, 2001. Pediatric Biomechanics. In: Nahum AM and J. Melvin, eds. Accidental Injury: Biomechanics and Prevention. Springer-Verlag, New York, NY, 550-587.

Yoganandan N, Pintar FA, Larson SJ, Sances A, Jr. eds, 1998, "Frontiers in Head and Neck Trauma: Clinical and Biomechanical," IOS Press, The Netherlands, 743 pp.

Yoganandan N, Pintar FA, Maiman DJ, Cusick JF, Sances A, Jr., Walsh PR, 1996. Human head-neck biomechanics under axial tension. Med Eng Phys 18(4), 289-94.

Yoganandan N, Pintar FA, Stemper BD, Baisden JL, Aktay R, Shender BS, Paskoff G, 2006. Bone mineral density of human female cervical and lumbar spines from quantitative computed tomography. Spine (Phila Pa 1976) 31(1), 73-6.

Yoganandan N, Pintar FA, Stemper BD, Baisden JL, Aktay R, Shender BS, Paskoff G, Laud P, 2006. Trabecular bone density of male human cervical and lumbar vertebrae. Bone 39(2), 336-44.

Yoganandan N, Stemper B, Kaufman B, Pintar F, 2008. Biomechanics of the Pediatric Spine. In: D. Kim, R. Betz, S. Huhn and P. Newton, eds. Surgery of the Pediatric Spine. Thieme, New York, NY, 11-22.

Yousefzadeh D, El-Khoury G, Smith W, 1982. Normal sagittal diameter and variation in pediatric cervical spine. Ped Radiol 144(2), 319-325.